REGULAR ARTICLE

blood advances

A mouse model characterizes the roles of ZIP8 in systemic iron recycling and lung inflammation and infection

Vida Zhang,[1,2] Supak Jenkitkasemwong,[3] Qingli Liu,[3] Tomas Ganz,[1] Elizabeta Nemeth,[1] Mitchell D. Knutson,[3,*] and Airie Kim[1,*]

[1]Department of Medicine, David Geffen School of Medicine, University of California, Los Angeles, Los Angeles, CA; [2]Department of Molecular and Medical Pharmacology, University of California, Los Angeles, Los Angeles, CA; and [3]Food Science and Human Nutrition Department, University of Florida, Gainesville, FL

Key Points

- ZIP8 knockout mice have elevated spleen iron levels and relative hypoferremia, suggesting that ZIP8 plays a role in iron recycling.
- Although lung ZIP8 is induced with inflammation, ZIP8 deletion in mice did not exacerbate acute lung injury or bacterial pneumonia.

ZIP8 (SLC39A8) is a transmembrane divalent metal ion importer that is most highly expressed in the lung and is inducible by inflammatory stimuli. In addition to zinc and manganese, ZIP8 can transport iron, but its specific roles in iron regulation during homeostatic and pathologic processes remain poorly understood. Using a novel global inducible ZIP8 knockout (KO) mouse, we analyzed the role of ZIP8 in steady-state iron homeostasis and during inflammation and infection. We observed an unexpected phenotype of elevated spleen iron levels and decreased serum iron in ZIP8 KO mice, suggesting that ZIP8 plays a role in iron recycling. We also showed that ZIP8 is expressed on lung distal airspace epithelial cells and transports iron from the airway into lung tissue. LPS-induced inflammation induced ZIP8 expression in the lung, but ZIP8 deletion had no detrimental effect on the severity of LPS-induced acute lung injury or on the outcomes of *Klebsiella pneumoniae* lung infection. Thus, ZIP8 plays a role in systemic iron homeostasis but does not modulate the severity of inflammatory lung injury or the host defense against a common bacterial cause of pneumonia.

Introduction

Iron is an essential trace mineral for normal cellular function in all living organisms, including DNA replication, cellular metabolism, and adenosine triphosphate generation. The largest fraction of iron in humans and other mammals is used for hemoglobin (Hb) synthesis and erythrocyte production. Low iron levels most commonly lead to insufficient red blood cell (RBC) production, causing anemia and impaired oxygen delivery to tissues. Excessive iron is also detrimental, leading to tissue damage as a result of excessive reactive oxygen species (ROS) generation by the Fenton reaction. Thus, iron homeostasis has evolved for tight iron regulation.

In humans, iron is primarily obtained from the diet, particularly from foods rich in heme. Iron is taken up in the duodenum and released on the basolateral side of enterocytes into the blood through ferroportin, the only known cellular iron exporter.[1] As free iron is dangerous because it generates ROS through the Fenton reaction, it is quickly taken up by the iron transporter transferrin in the blood so that it can be safely transported to tissues. Iron-laden transferrin binds to transferrin receptor 1 (TFR1) on cell

Submitted 15 April 2022; accepted 12 September 2022; prepublished online on *Blood Advances* First Edition 19 October 2022. https://doi.org/10.1182/bloodadvances.2022007867.

*M.D.K. and A.K. contributed equally to this study.

Data are available on request from the corresponding author, Airie Kim (airiekim@mednet.ucla.edu).

The full-text version of this article contains a data supplement.

surfaces and is internalized, allowing iron to be used by the cell.[2] Unused intracellular iron is stored in the iron storage protein ferritin until needed. Most of the body's iron is used by erythroid precursor cells in the bone marrow to make RBCs.[3] As the RBCs age or are damaged, they are phagocytosed by macrophages residing in the red pulp. The macrophages extract iron from Hb and release it into circulation through ferroportin.[4] Excess body iron is stored in the liver, the main iron storage organ, and is mobilized when iron demand is high. Hepcidin, a peptide hormone produced in the liver, is the master regulator of systemic iron homeostasis and functions by binding to ferroportin and causing its internalization and degradation.[1]

Regulation of extracellular iron concentration plays an important role in host defense. Numerous studies have defined the detrimental effect of iron overload in infections by multiple pathogens, including *Yersinia enterocolitica*, *Escherichia coli*, and *Klebsiella pneumoniae*.[5-8] Multiple host defense pathways function to sequester iron away from pathogens. Hepcidin-mediated hypoferremia during infections is an important form of nutritional immunity.[1,8] Neutrophil gelatinase–associated lipocalin prevents bacterial iron uptake by sequestering siderophores, bacterial compounds that bind to iron for active uptake by the microbe.[9] Lactoferrin is present in the mucosa and functions similarly to transferrin by binding to iron for reuptake through lactoferrin receptors.[10] Intracellularly, natural resistance–associated macrophage protein 1 is expressed in macrophage phagosomes and reduces iron availability for various intraphagosomal pathogens.[11]

In addition to systemic iron regulation, cells and tissues also regulate iron in an autocrine/paracrine manner, although these mechanisms are less well understood. In the lungs, iron regulation has multiple unique challenges. The lung epithelium is exposed to external air as part of its role in air-blood gas exchange, which also exposes it to iron particles and infectious pathogens that can potentially cause injury.[12,13] In addition, altered iron levels have been associated with lung pathologies such as acute lung injury (ALI), chronic obstructive pulmonary disease, and pulmonary hypertension.[12] However, how iron uptake and distribution is regulated in the lung remains unclear.

ZIP8 (SLC39A8) is a transmembrane divalent metal transporter that was initially identified as a zinc importer but has since been shown to transport manganese as well as iron with high affinity.[14-16] In humans, ZIP8 mutations are associated with schizophrenia, Crohn's disease, and manganese deficiency.[17-19] However, its roles in iron homeostasis and related pathology have yet to be determined. Interestingly, ZIP8 is most highly expressed in the lung compared with other tissues, and is also more highly expressed in the lung than known iron transporters, such as ZIP14, DMT1, and TFR1.[15] In addition, ZIP8 is induced by inflammation, including that caused by lipopolysaccharides (LPS) and tobacco smoke, which suggests that ZIP8 may play a role in lung host defense through iron regulation.[20-22] Our goal was to determine the physiological functions of ZIP8 in iron homeostasis and investigate the role of ZIP8 in pulmonary host defense.

Here, we report the characterization of a novel global ZIP8 knockout (KO) mouse during homeostasis and pathologic conditions. The iron characterization studies were performed in parallel in 2 separate laboratories, the Kim lab at the University of California, Los Angeles (UCLA) and the Knutson lab at the University of Florida (UF), using the same genetic mouse model. Although minor variations in phenotype were observed between laboratories, the effects of ZIP8 deletion were substantially similar between both groups, strengthening the conclusions of our findings.

Methods

Refer to the supplemental figure legends for UF materials and methods.

Animal models

C57BL/6 (B6) mice were purchased from Jackson Laboratories (JAX # 000664). Conditional-ready, ZIP8 floxed allele ($ZIP8^{fl/fl}$) mice were generated from mice harboring a targeted recombinant allele (*r*) of *Slc39a8* (C57BL/6NTac-$Slc39a8^{tm1a(EUCOMM)Wtsi/Cnrm}$; European Mouse Mutant Archive). Briefly, the *r* allele harbors *LoxP* recombination sites flanking exon 3 of the *Slc39a8* gene and *FRT* sites flanking a neomycin resistance gene (*neo*) adjacent to the upstream *LoxP* site. To delete the neo cassette and generate $ZIP8^{fl/fl}$ mice, $Slc39a8^{+/r}$ mice were bred with ROSA26:FLPe knockin mice with ubiquitous expression of FLP1 recombinase (B6.129S4-Gt(ROSA)26$Sor^{tm1(FLP1)Dym}$/RainJ; The Jackson Laboratory, JAX# 009086). Polymerase chain reaction and DNA sequencing of $ZIP8^{fl/fl}$ mice verified deletion of the *FRT*-flanked sequence and confirmed the *LoxP* sites flanking exon 3. To generate ZIP8 KO mice, $Slc39a8^{fl/fl}$ mice were bred with mice expressing tamoxifen-inducible Cre under the Gt(ROSA)26Sor promoter ($iRosaCre^{+/-}$; Jackson Laboratory, JAX #008463) to generate $iRosaCre^{+/-}$;$ZIP8^{fl/fl}$ and $iRosaCre^{-/-}$;$ZIP8^{fl/fl}$ littermates. At 4 weeks of age, $iRosaCre^{+/-}$;$ZIP8^{fl/fl}$ mice were placed on a 500 mg tamoxifen per kg diet (Teklad; 80 mg/kg body weight per day) for 2 weeks to induce Cre-mediated recombination and ZIP8 gene excision, then placed back on regular chow to regain weight. These mice are referred to as ZIP8 KO mice (deletion of ZIP8 confirmed in supplemental Figure 1). $iRosaCre^{-/-}$;$ZIP8^{fl/fl}$ littermates were placed on the same diet regimen as controls. Age- and sex-matched male and female mice that were 14 to 64 weeks old were used in experiments. Mice of both sexes were used for experiments.

To assess the response of splenic ZIP8 induction to iron, 8-weeks-old B6 mice were injected with 300 μL aged RBCs, a single intraperitoneal (IP) injection of 10 mg iron dextran (MilliporeSigma, D8517) or 2 consecutive daily doses of 60 mg/kg phenylhydrazine hydrochloride (PHZ, Sigma 114715). To obtain aged RBCs, mouse blood was collected into heparin-containing tubes, then diluted in sterile phosphate-buffered saline (PBS) and centrifuged to remove the plasma and buffy coat. The cells were washed again in PBS, counted, and resuspended in HEPES buffer (10 mM HEPES, 140 mM NaCl, BSA 0.1%, pH 7.4) to 10^8 RBC per mL. RBCs were aged by adding calcium and Ca2+ ionophore A23187 to a final concentration of 2.5 mM and 0.5 μM, respectively, then incubating at 30°C for 16 hours. Aged RBCs were washed with PBS and counted before use.

To induce hemolytic anemia, ZIP8 KO mice and littermate controls were injected IP with 60 mg/kg PHZ (dissolved in PBS) on day 0 and day 1. Complete blood counts (CBCs) were measured on day 4 via cheek bleed, the peak of hemolytic anemia severity, and on day 7, post recovery. On day 7, mice were euthanized and tissues were harvested for analysis. During the PHZ course, mice were placed on a 4 ppm Fe diet to minimize uptake of dietary iron.

For iron deficiency studies, ZIP8 KO mice and littermate controls were placed on a low-iron diet (4 ppm iron; TD 80396, Envigo) at 8 weeks of age for up to 24 weeks to induce iron deficiency. Blood was collected via cheek bleeds and CBCs were assessed every 4 weeks.

To induce ALI, mice were treated with 15 mg/kg LPS (Sigma, E. coli O55:B5, L2880) in saline through oropharyngeal (OP) aspiration, which was modified from.[23] In brief, mice were anesthetized with an IP injection of ketamine/xylazine (Sigma-Aldrich), then suspended on a wire by the front incisors. After placement of a nose clip, the tongue was gently pulled out of the mouth and to the side using forceps. The LPS solution was then pipetted into the posterior OP space, and the nose and tongue were released 5 seconds after the solution is aspirated into the lungs. The dose of 15 mg/kg LPS was used after a titration study for the lowest dose necessary to consistently yield evaluable ALI parameters. Mice were euthanized 3 days after LPS treatment, and bronchoalveolar lavage (BAL) fluid was obtained by lavaging the lungs 3 times with 0.8 mL of cold PBS. Lungs were perfused with 5 mL of cold PBS via the right ventricle, then lungs and liver were harvested and snap frozen in liquid nitrogen for analysis. BAL fluid protein was measured using the Pierce BCA Protein Assay Kit (Thermo Fisher).

For *K pneumoniae* infection experiments, bacteria were purchased from ATCC (BAA-1705). Before the experiment, an aliquot of the stock was thawed and cultured in tryptic soy broth overnight at 37°C, then reinoculated into fresh media and allowed to reach linear growth phase. The bacteria were then spun down and resuspended in PBS, then diluted to the desired concentration as determined by an OD600 vs colony forming units (CFU) curve for the specific strain. Mice were infected with 300 CFU of K. pneumoniae via OP aspiration and weighed daily until euthanasia 3 days later. Blood was collected via cardiac puncture and tissues and BAL fluid were harvested for analysis. Bacterial burden was measured by homogenizing tissue in sterile water or diluting blood with sterile water and plating serial fivefold dilutions on blood agar plates (Fisher, R01200). The plates were incubated at 37°C for 15 to 16 hours, and the number of colonies was counted.

CBCs were measured from whole blood (mixed with 1 μL of heparin to prevent clotting) using a HemaVet blood analyzer (Drew Scientific).

Iron assay

Nonheme iron concentrations were determined by a colorimetric assay for iron quantification (Sekisui Diagnostics). For mouse tissue samples, tissues were flash frozen and ground up in liquid nitrogen to homogenize the samples. Approximately 40 mg of tissue was weighed and digested in a fixed volume of acid (3M HCl, 10% trichloroacetic acid) for 1 hour at 95°C. Samples were centrifuged to clear the insoluble material, and then iron levels in the supernatant were quantified according to the manufacturer's instructions. For mouse serum samples, blood was collected via cardiac puncture and placed in serum separator tubes (BD, 365967), then centrifuged to separate serum from RBCs according to the manufacturer's instructions. Using the same assay, 10 μL of serum was used to determine the concentration of iron in the serum.

Histology/immunohistochemistry (IHC)

Mouse spleens were harvested and fixed in 10% neutral-buffered formalin for 24 hours at room temperature, then stored in 70% ethanol until processing. The tissues were paraffin-embedded and sectioned at 4 μm thickness by the UCLA Translational Pathology Core Laboratory. Normal human lung tissue was obtained from Borna Mehrad (UF) and processed at UCLA. Before staining, sections were heated for 45 minutes at 50°C and deparaffinized through serial changes of xylene and ethanol and rehydrated to distilled water. Light microscopy images were captured by a digital camera (SPOT Imaging).

For iron localization, mouse spleen tissues underwent enhanced Perls' stain using potassium ferrocyanide 2% and HCl 4% and the Vector SG Peroxidase Substrate Kit (Vector Laboratories; SK-4700) and were then counterstained with 0.5% neutral red solution.

For IHC for ZIP8 and SP-C in human lung tissue, antigen retrieval was performed by boiling in Tris-EDTA (10 mM Tris base 1 mM disodium EDTA dihydrate, pH 9.0) for 10 min. IHC was performed using ImmPRESS HRP Goat Anti-Rabbit IgG Polymer Detection Kit, Peroxidase (MP-7451) and ImmPRESS-AP Horse Anti-Mouse IgG Polymer Kit, Alkaline Phosphatase (MP-5402) according to the manufacturer's instructions, with rabbit anti-ZIP8 rabbit antibody (Sigma HPA038833) and mouse anti-SP-C antibody (Santa Cruz, sc-518029) used as the primary antibody at 200 ng/mL. Negative control sections were incubated with normal rabbit and mouse IgG at the same concentration. HRP was developed using ImmPACT DAB Substrate, Peroxidase (HRP) (SK-4105) according to the manufacturer's instructions. Alkaline phosphatase was developed using the ImmPACT Vector Red Alkaline Phosphatase Substrate Kit (SK-5105). Sections were counterstained with Gill's hematoxylin. All reagents for IHC were purchased from Vector Laboratories unless stated otherwise.

Magnetic cell sort

Unless otherwise stated, all reagents for the magnetic bead separation were purchased from Miltenyi. Mouse spleens were minced using the frosted side of microscope slides, rinsed with protein extraction buffer (PEB), and filtered through a 40 μm filter to obtain single-cell suspension. Cells were incubated with F4/80 MicroBeads (magnetic beads bound to anti-CD45 antibodies) and flowed through an LS column placed in QuadroMACS magnet according to the manufacturer's instructions to obtain F4/80+ and F4/80- cell populations.

Mouse lungs were lavaged with PEB (PBS pH 7.2, 2mM EDTA, 0.5% BSA) to obtain BAL fluid. Lungs were perfused via right cardiac ventricle with 10 mL of cold PBS, then digested using the Lung Dissociation Kit and gentleMACS Dissociator per manufacturer's protocol, and a single-cell suspension will be obtained by filtering cells through a 40 μm filter. Airway alveolar macrophages were obtained by isolating CD45+ cells from BAL fluid. From the lungs, a sequential negative selection was performed to obtain a CD45+ population (immune cells), CD45-CD31+ population (endothelial cells), and CD45-CD31-Epcam+ population (epithelial cells). In brief, cells were incubated with CD45 MicroBeads, then flowed through an LS column placed in QuadroMACS magnet.

CD45+ cells were bound to the column, whereas CD45- cells were in the flow through. The CD45+ cell population was obtained by flushing the column with PEB after it was removed from the magnet. This process was repeated to obtain CD31+ cells from the CD45- population and Epcam+ cells from the CD45-CD31- population using MicroBeads bound to the respective antibodies.

Quantitative polymerase chain reaction

Tissue RNA was extracted via TRIzol (Thermo Fisher Scientific), and cDNA was synthesized using the iScript cDNA Synthesis Kit (BioRad). Gene transcript levels were quantified in duplicate by SsoAdvanced Universal SYBR Green Supermix (BioRad) using a CFX Connect or CFX96 Touch Real-Time PCR Detection System (BioRad). Messenger RNA (mRNA) expression was calculated using the ΔCT method normalized to hypoxanthine guanine phosphoribosyl transferase (Hprt) expression levels. Primers are listed in supplemental Table 1.

Western blot

Frozen ground tissue or cells were homogenized in RIPA buffer containing protease and phosphatase inhibitors. Protein concentration in tissue lysates was determined by a BCA assay (ThermoFisher Pierce, 23225), and then lysates were denatured by sodium dodecyl sulfate (SDS) and boiling. For ferroportin, lysates were not denatured by SDS and not boiled. Approximately 15 mg of protein were loaded per lane and were separated by SDS polyacrylamide gel electrophoresis and transferred to nitrocellulose membranes. Membranes were blocked for 1 hour in 5% w/v dried nonfat milk and incubated with primary antibodies in primary antibody dilution buffer (20 mM Tris pH 8, 200 mM NaCl, 0.25% Tween 20, 2% BSA, 0.1% NaN_3) overnight at 4°C. The secondary reaction was performed using HRP-conjugated anti-rabbit or anti-mouse IgG diluted in blocking buffer. Protein blots were visualized by chemiluminescence using the ChemiDoc XRS+ imaging system and quantified using Image Lab software (BioRad).

Commercial antibodies used are listed in supplemental Table 2. Monoclonal mouse anti-ZIP8 antibody (9D4A9) was generated and purified by Genscript using the antigen protein sequence: MHPSEGPELAFSEDVLSVFGANRSLSAAQLGRLLERLGAASQQ GALDLGQLHFNQCLSAEDIFSLHGFSNVTQITSSNFSAICPAILQ QLNFHPCEDLRKHNAKPSHHHHHH.

Cell lines

A549 cells (ATCC, CCL-185) and 16HBE cells (Sigma, SCC150) were cultured in RPMI 1640 medium with GlutaMAX supplement (Thermofisher, 61870036), supplemented with 10% FBS and 1× Pen/Strep, at 37°C in a 5% CO_2 95% air atmosphere. For experiments, cells were seeded at 2×10^5 per well in 12-well plates and allowed to adhere overnight. Cells were serum-starved (complete media with 0.1% FBS) for 24 hours, then treated with 50 ng/mL recombinant human interleukin-6 (IL-6) (R&D Systems #206-IL), interferon gamma (PeproTech #300-02), IL-1α (PeproTech #200-01 A), IL-1β (PeproTech #200-01B), tumor necrosis factor α (TNFα) (Biolegend #570102) or epidermal growth factor (Gibco #10450). Cells were harvested for analysis 16 hours after treatment. ZIP8 knockdown was performed using Lipofectamine RNAiMAX Reagent (Invitrogen, 13778150) and Opti-MEM according to the manufacturer's instructions. OnTarget Smart Pool siRNAs targeting human ZIP8 (L-007573-01-0005) or nontargeting control siRNA (D-001810-10-05) were purchased from Horizon Discovery.

^{58}Fe isotope preparation and sample analysis

^{58}Fe (93% enrichment) was purchased from Trace Sciences International, dissolved in 12N HCl to form H_2 plus $^{58}FeCl_2$, and H_2O_2 was added to oxidize the H_2 plus $^{58}FeCl_2$ to H_2O plus $^{58}FeCl_3$. 100 mM of $^{58}FeCl_3$ in 12N HCl was diluted 1:400 in 10 mM of sodium ascorbate to obtain ferrous $^{58}Fe^{2+}$. ZIP8 KO mice and littermate controls were treated with 5 μg of $^{58}Fe^{2+}$ via retroorbital (RO) injection or OP aspiration. After 4 hours, the mice were euthanized, and lung tissue and BAL fluid were collected for analysis. Acid extraction to extract nonheme iron was performed on lung tissues as listed above, and supernatant and BAL fluid were submitted to the UCLA ICP-MS Core Facility for ICP-MS analysis of ^{56}Fe and ^{58}Fe.

Tissue concentrations of other metals were also determined at the UCLA ICP-MS facility within the UC Center for Environmental Implications of Nanotechnology.

Myeloperoxidase (MPO) assay

A quantity of ~10 mg of ground lung tissue was weighed and homogenized in 50 mM potassium phosphate solution, pH 6.0. The solution was centrifuged, then the pellet was resuspended in 0.5% CETAB in Cell-Based Assay Buffer (Cayman #10009322). After sonication and incubation, MPO activity in the supernatant was measured using the colorimetric neutrophil MPO activity assay kit (Cayman #600620). BALF MPO activity was measured directly with the assay kit. MPO activity was measured as the rate of change of absorbance over time.

Superoxide dismutase (SOD) assay

SOD was assessed in tissues using the Superoxide Dismutase Assay Kit (Cayman Chemicals, #706002) following the manufacturer's instructions.

Malondialdehyde assay

Malondialdehyde was quantified in mouse tissues as a measure of lipid peroxidation using the Thiobarbituric Acid Reactive Substances (TCA Method) Assay Kit (Cayman Chemicals #700870) following the manufacturer's instructions.

Statistics

Graphpad Prism (version 9.0 for Windows, GraphPad Software) was used for all statistical analyses. Normally and nonnormally distributed data were analyzed using the *t* test or Mann-Whitney rank-sum test, respectively. Multivariate analyses were performed using 2-way analysis of variance.

Study approval

All animal experiments were approved by the UCLA Institutional Animal Care and Use Committee and were carried out in accordance with the Guide for Care and Use of Laboratory Animals (National Institutes of Health, Bethesda, MD). All mice were maintained on a 12-hour light-dark schedule in a temperature- (22-25°C) and humidity-controlled environment. Unless specified, mice received a standard diet (PicoLab Rodent Diet 20, 5053 Irradiated, 185 ppm iron). At the end of experiments, mice were humanely euthanized using CO_2 inhalation.

Results

Metal analysis of baseline ZIP8 KO mice

As whole-body deletion of ZIP8 is embryonic lethal, and ZIP8 hypomorphic mice do not survive beyond postnatal day 2,[24,25] we generated an inducible whole-body ZIP8 KO mouse to characterize the role of ZIP8 in vivo (supplemental Figure 1A). Loss of ZIP8 was confirmed at the DNA, RNA, and protein levels (supplemental Figure 1B-D). Mice appeared phenotypically normal up to at least 1 year of age. In addition, we used a custom-made in-house antibody targeting mouse ZIP8 that outperformed multiple commercial antibodies in our verification assays.

We performed ICP-MS on various tissues from 16-week-old ZIP8 KO and littermate controls to quantify any baseline differences in the levels of iron (heme + nonheme), zinc, and manganese (Mn). In the liver, there were no significant differences in iron or zinc concentrations, but ZIP8 KO mice did have significantly less Mn compared with their controls (Figure 1A-B), as has been previously reported.[26] In the spleens, no difference in zinc levels was observed, though there was a noticeable but not statistically significant decrease in manganese levels in the ZIP8 KO spleens. Unexpectedly, ZIP8 KO spleens also had significantly more iron (both concentration and total) than their littermate controls (Figure 1C-D).

ZIP8 KO mice have impaired iron recycling

To determine the cause of this increased iron in ZIP8 KO spleens, we analyzed steady-state iron and hematological parameters of 16-week-old ZIP8 KO mice at UCLA and 16- and 12-week-old mice at UF. Tissue nonheme iron measurements by colorimetry confirmed no significant difference in liver iron levels between the 2 groups and significantly higher spleen iron levels in ZIP8 KO mice at both institutions (UCLA: fl/fl 298 μg Fe/g tissue vs KO 516 μg Fe/g tissue, $P < .0001$) (Figure 2A and supplemental Figure 2A,C). Accordingly, the KO mice at both institutions had lower serum/plasma iron levels, suggesting that decreased circulating iron results from increased splenic iron sequestration. At UCLA, despite the apparent reduced iron availability for erythropoiesis, there was no significant difference in baseline Hb, hematocrit (HCT), or mean corpuscular volume (MCV) between ZIP8 KO and control littermates (Figure 2B). At UF, ZIP8 KO mice at 16 weeks of age had a mildly decreased Hb (fl/fl 13.47 g/dL vs KO 12.13 g/dL, $P < .005$) and increased reticulocyte count (fl/fl 1.36% vs KO 4.51%, $P < .001$), indicating impaired erythropoiesis secondary to splenic iron sequestration and reduced iron availability (supplemental Figure 2B). A similar decrease in Hb concentrations was also observed in a larger cohort of mice at 12 weeks of age (supplemental Figure 2D). The manifestation of the mild erythropoietic impairment could potentially be a result of institutional differences in the vivarium environment, such as different diets, use of metal cages, etc. Nonetheless, splenic iron sequestration and hypoferremia were consistently observed in the ZIP8 KO mice in both laboratories. These differences in splenic and serum iron were also observed in >1-year-old ZIP8 KO mice and littermates, though Hb was also mildly elevated in aged ZIP8 KO mice (supplemental Figure 3A-B). Analysis of the systemic regulators of iron homeostasis showed that liver hepcidin and bone marrow erythroferrone (*Erfe*, hepcidin regulator) mRNA levels were unchanged in KOs compared with control mice (Figure 2C), consistent with the lack of difference in liver iron concentrations or CBCs between the 2 genotypes (at UCLA). Perls' staining of the spleen showed that the increased iron was in the red pulp of the spleen (Figure 2D), the site of erythrocyte turnover.[27] Using magnetic cell sorting, we confirmed that spleen ZIP8 is primarily expressed in red pulp macrophages (CD45+), the specific cells responsible for iron recycling from senescent and damaged RBCs[27] (Figure 2E). Taken together, these data suggest that ZIP8 is involved in erythrocyte turnover and iron recycling.

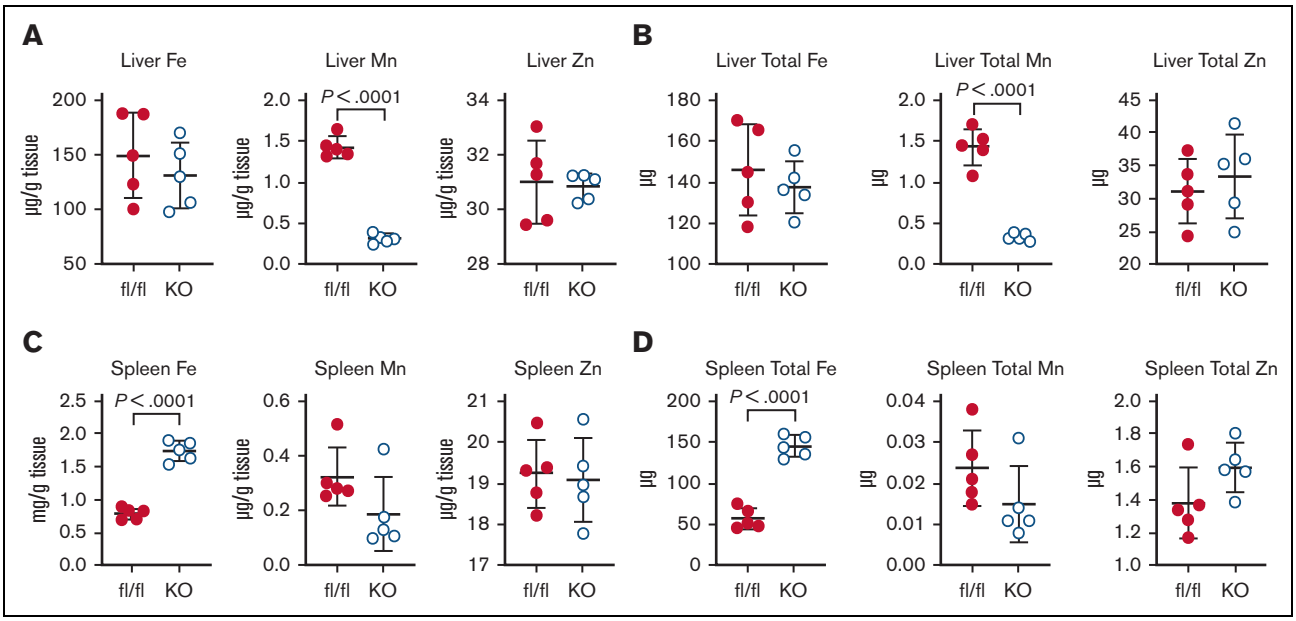

Figure 1. ZIP8 KO mice have decreased liver manganese and increased splenic iron levels. ICP-MS was performed on liver and spleens from 16-week-old ZIP8 KO mice and littermate controls (fl/fl). n = 5 mice per group. (A,C) Concentrations and (B,D) total levels of (A-B) liver and (C-D) splenic iron, manganese, and zinc were measured. Graphs depict mean and SD; *P* values determined by 2-tailed unpaired Student *t* test. SD, standard deviation.

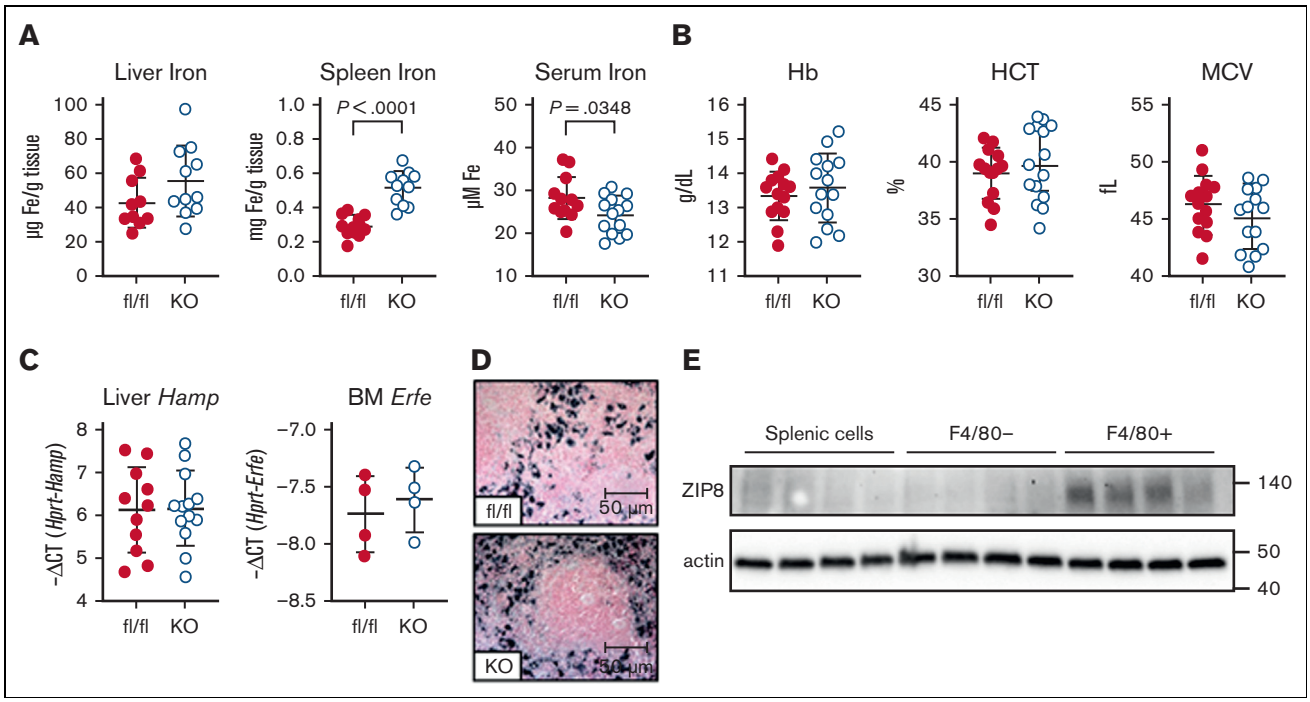

Figure 2. Baseline ZIP8 KO mice have impaired iron recycling. (A-D) Tissues and serum from 16-week-old ZIP8 KO and littermate controls (fl/fl) were harvested for analysis. n = 4 to 14 mice per group. (A) Liver, spleen and serum nonheme iron levels. (B) CBCs. (C) Liver *Hamp* mRNA and BM *Erfe* mRNA levels. (D) Representative images of Perls' staining for iron in ZIP8 KO and fl/fl FFPE spleen tissue. 40× original magnification. (E) Splenic red pulp macrophages from C57BL/6 mice were isolated via magnetic bead selection for F4/80+ cells. ZIP8 protein levels are enriched in the splenic F4/80+ population as determined by western blot. n = 4 mice per group. (A-C) Graphs depict mean and SD; *P* values determined by 2-tailed unpaired Student *t* test. BM, bone marrow; FFPE, formalin-fixed paraffin-embedded; SD, standard deviation.

Interestingly, despite higher nonheme iron concentrations in the KO spleen, there were no changes in the *Tfr1* mRNA expression or ferroportin and ferritin protein levels. In addition, there was no difference in the mRNA levels of *Hmox*, the enzyme responsible for the first step of heme degradation (supplemental Figure 4A-B). There was also no evidence of downstream oxidative damage in KO mice, as shown by unchanged spleen malondialdehyde levels and *Nqo1* expression (supplemental Figure 4C).

ZIP8 deletion does not modify hemolytic anemia

To evaluate whether ZIP8 has a role during conditions of accelerated erythrophagocytosis and iron recycling, we used mouse models of parenteral iron administration, erythrophagocytosis of aged RBCs, and PHZ-induced hemolytic anemia. 8-weeks-old C57BL/6 (B6) mice were injected IP with 10 mg iron dextran, 300 µL packed aged RBCs, or 60 mg/kg PHZ daily for 2 days, and the spleens were harvested 3 days after treatment. Splenic ZIP8 protein levels were induced in response to iron dextran as well as to PHZ (at both institutions) (Figure 3A and supplemental Figure 5A) but not in response to aged RBCs. The amount of ZIP8 protein across different conditions positively correlated to the amount of iron present in the spleen (Figure 3B). However, the inflammatory marker Saa1 was also induced in response to iron dextran and PHZ (3 days after treatment, Figure 3C), suggesting that the increase in ZIP8 expression could be secondary to increased inflammation rather than iron status or accelerated erythrocyte turnover.

PHZ-treated mice had CBCs measured on day 4, the peak of hemolytic anemia severity, and on day 7, post recovery. We found no significant differences in RBC, Hb, HCT, or MCV levels between ZIP8 KO mice and their controls on day 4 or day 7 (Figure 3D and supplemental Figure 5B). There was also no change in inflammation and oxidative stress at day 7 as measured by liver *Saa1* and spleen *Nqo1* mRNA, respectively (Figure 3E). After PHZ treatment, ZIP8 KO mice had more splenic iron compared with their controls in both laboratories (Figure 3F and supplemental Figure 5C), despite an unchanged number of splenic macrophages as assessed by the expression of *Adgre,* gene encoding F4/80 (supplemental Figure 6B), and without a difference in serum iron levels (Figure 3F). We observed a small but statistically significant increase in spleen ferroportin protein levels in ZIP8 KO mice at UCLA but not at UF (supplemental Figure 6A,C). Taken together, these data suggest that although ZIP8 does increase in response to iron loading and hemolytic anemia, it does not appear to play a crucial role in recovery from hemolytic anemia.

Iron deficiency and ZIP8

We used a mouse model of iron deficiency to assess the role of ZIP8 in the mobilization of recycled iron. At UCLA, 8-week-old ZIP8 KO mice and littermate controls were placed on a 4 ppm iron diet for 24 weeks and underwent regular blood draws for CBC measurements until harvest. As expected, RBC, Hb, HCT, and MCV levels all decreased in both groups because of prolonged iron

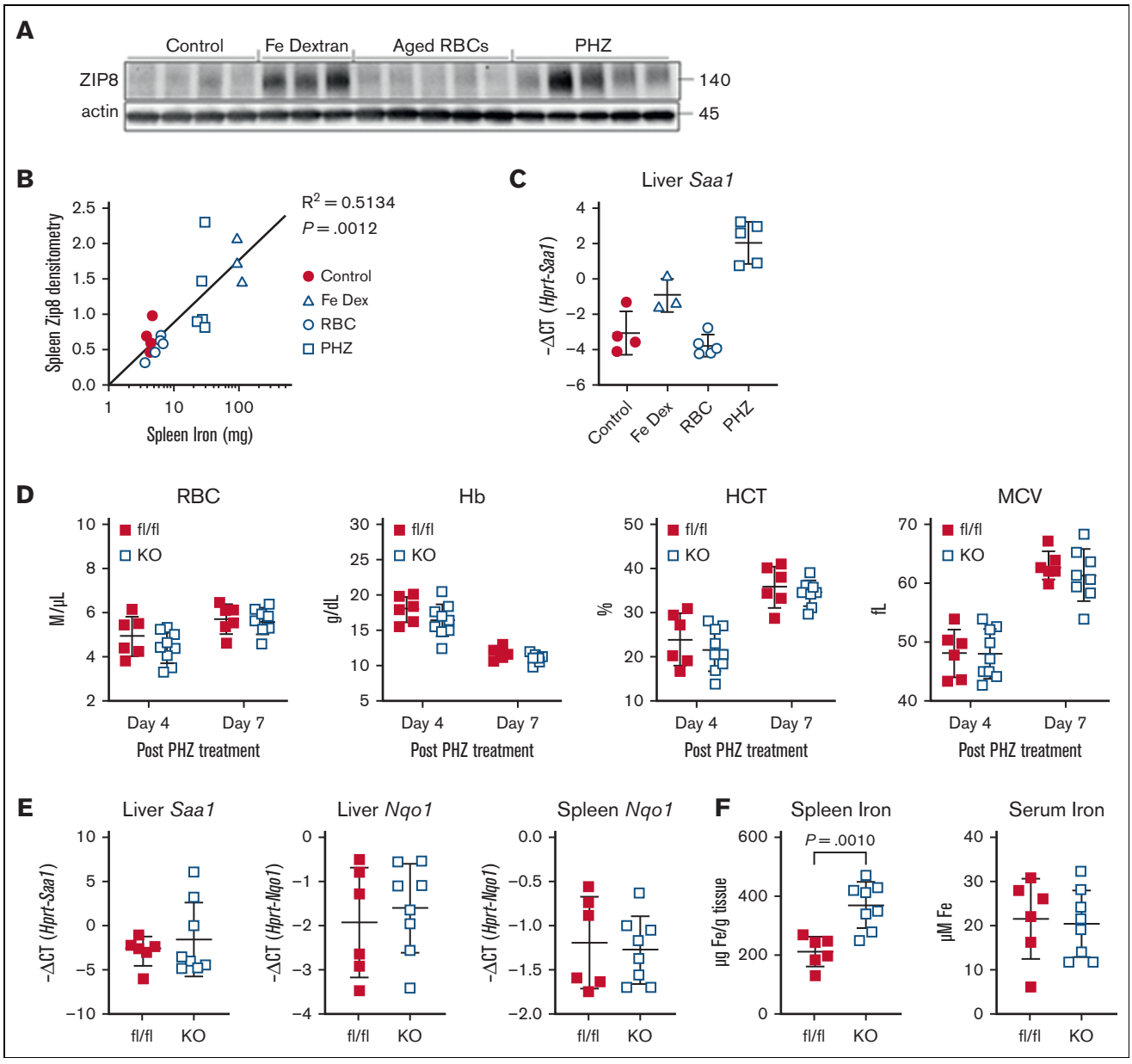

Figure 3. ZIP8 KO and WT mice have similar responses to PHZ. (A-C) C57BL/6 mice were treated with 300 μL of aged RBCs, a single IP injection of 10 mg iron dextran or 2 consecutive daily doses of 60 mg/kg PHZ to induce hemolytic anemia. n = 3 to 5 mice for each treatment group. Tissues were harvested 3 days after treatment. n = 3 to 5 mice per group. (A) Western blot of splenic ZIP8. (B) Correlation between splenic ZIP8 protein levels as quantified by densitometry and splenic nonheme iron levels. *P* value and R^2 as determined by Pearson's correlation. (C) Liver *Saa1* mRNA levels. (D-F) ZIP8 KO and littermate controls (fl/fl) were treated with PHZ as described above. n = 6 to 9 mice per group. (D) CBCs were performed on day 4 and day 7 on heparinized blood from ZIP8 KO and fl/fl mice. (E) Day 7 liver *Saa1*, liver *Nqo1*, and spleen *Nqo1* mRNA levels and (F) spleen and serum nonheme iron. (A,C-F) Graphs depict mean and SD; *P* values determined by 2-tailed unpaired Student *t* test. SD, standard deviation; WT, wild-type.

deficiency and repeated blood draws. However, there was no significant difference in CBC parameters between ZIP8 KO mice and littermate controls at any time point measured (Figure 4A). There was also no significant difference in zinc protoporphyrin, a marker of iron deficiency (Figure 4B), and iron measurements in serum, spleen, and liver showed no significant difference with ZIP8 deletion (Figure 4C). There was also no difference in the iron transporters ferroportin or TFR1, the iron storage protein ferritin, nor in liver *Hamp* (Figure 4D-E).

In a parallel experiment at UF, ZIP8 KO mice and littermates were fed an iron-deficient diet for 8 weeks. Although the short-term iron-deficient diet regimen did not decrease Hb levels in either control or KO mice (supplemental Figures 2B and 7A), liver nonheme iron concentrations were low in both groups, consistent with iron deficiency (supplemental Figure 7B). Splenic iron concentrations, however, were higher in ZIP8 KO mice than in control mice. The higher splenic iron levels in ZIP8 KO were associated with elevated ferritin levels in the spleen with no change in ferroportin protein

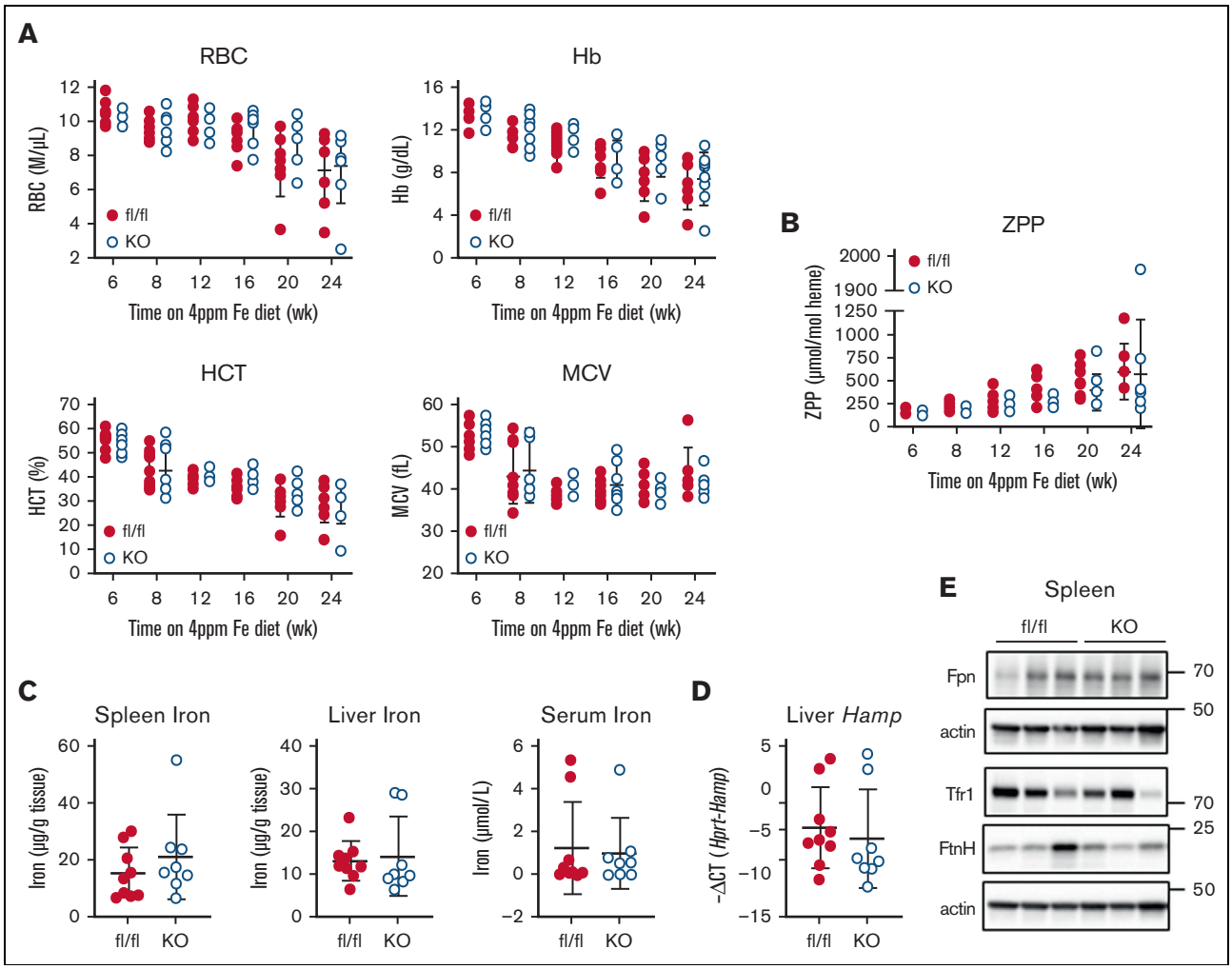

Figure 4. Loss of ZIP8 has no effect on response to iron deficiency in mice. ZIP8 KO mice and littermate controls (fl/fl) were placed on a 4 ppm Fe diet and CBCs were measured at 6, 8, 12, 16, 20, and 24 weeks on the diet. Tissues and serum were harvested at the end of the treatment. n = 8 to 9 mice per group. (A) CBCs from ZIP8 KO and fl/fl mice. (B) Blood ZPP levels. (C) Spleen, liver, and serum nonheme iron levels from iron-deficient ZIP8 KO mice and fl/fl mice. (D) Liver *Hamp1* mRNA. (E) Representative western blot for splenic Fpn, Tfr1, and FtnH protein. (A-D) Graphs depict mean and SD. SD, standard deviation; ZPP, zinc protoporphyrin.

levels (supplemental Figure 7C). Interestingly, although splenic nonheme iron was higher in ZIP8 KOs, TFR1 levels were paradoxically increased compared with the controls (supplemental Figure 7C-D). It is possible that the increased ferritin levels reflect macrophage iron status, whereas increased TfR1 levels reflect an increase in extramedullary hematopoiesis resulting from impaired iron availability. Indeed, expression of several erythropoietic markers increased in ZIP8 KO compared with wild-type spleens (*Alas2, Erfe, Mfrn1*, supplemental Figure 7D).

Taken together, our data suggest that after a short exposure to iron deficiency, ZIP8 KO mice still retained iron in the spleen. However, after prolonged iron deficiency, together with repeated blood draws, iron was effectively mobilized and no difference in CBCs was observed, suggesting that ZIP8 does not play a major role in the increased iron mobilization and handling that occurs during the stress state of iron deficiency.

ZIP8 is expressed in alveolar epithelial cells and is induced by inflammation

ZIP8 is most highly expressed in the lung compared with other tissues in the body, but no studies have systematically examined the role of ZIP8 in lung iron regulation. Using IHC on normal human lung tissue sections, we found that ZIP8 is expressed on the apical side of AT1 and AT2 cells facing the air-filled compartment (Figure 5A) and not expressed on endothelial cells.

There have been reports in the literature that ZIP8 is inducible by various inflammatory stimuli,[20-22] and we confirmed this in human cells in vitro. We treated A549 (a human alveolar epithelial cell line) with various cytokines and growth factors. ZIP8 mRNA and protein were induced after treatment with IL-1a, IL-1b, and TNFα (Figure 5B-C). The specificity of ZIP8 detection was confirmed through siRNA knockdown of ZIP8 (Figure 5D). ZIP8 induction with inflammatory stimuli appears to be specific to alveolar

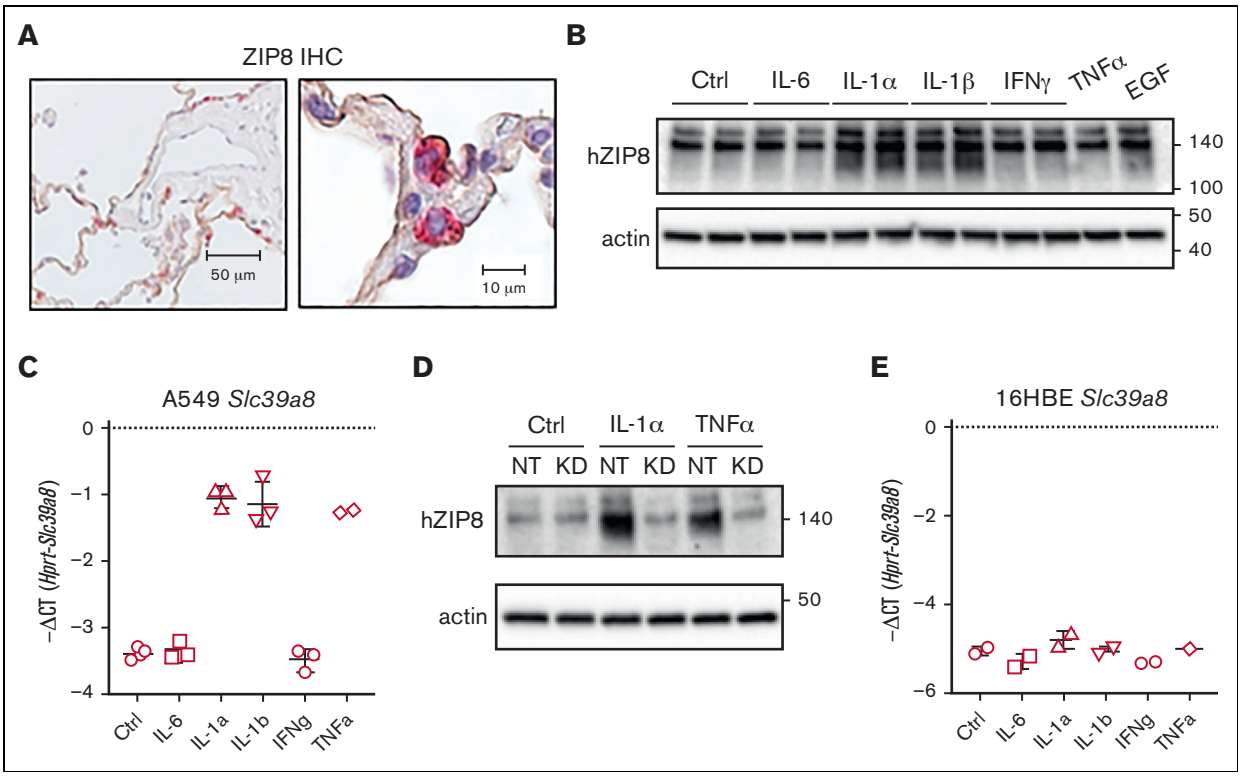

Figure 5. ZIP8 is induced by inflammation in human alveolar epithelial cells. (A) Representative images for IHC for ZIP8 (brown) and SP-C (red; AT2 cells) in normal human lung tissue (n = 2 biological replicates). Images are 10× (left) and 40× (right) original magnification. (B-D) A549 cells (human alveolar epithelial cell line) were serum starved for 24 hours, then treated with 50 ng/mL recombinant human IL-6, IFN-γ, IL-1α, IL-1β, TNFα, or epidermal growth factor for 16 hours. n = 1 to 3 independent experiments. (B) Representative western blot for ZIP8 protein expression. (C) *SLC39A8* mRNA levels. (D) ZIP8 siRNA knockdown. (E) 16HBE cells (human bronchiolar epithelial cell line) *SLC39A8* mRNA levels after treatment for 16 hours. Graphs depict mean and SD. IFN- γ, interferon gamma; KD, ZIP8 siRNA; NT, nontargeting siRNA; SD, standard deviation.

epithelial cells, as there was no ZIP8 increase in HBECs (a human bronchiolar epithelial cell line) with identical stimuli (Figure 5E).

ZIP8 transports iron from the airspace to the lung

As there was no existing literature describing the in vivo function of ZIP8 in lung iron homeostasis, we used ZIP8 KO mice to investigate the location and directionality of ZIP8-mediated iron transport. Using magnetic sorting of mouse lung cells, we found that *Slc39a8* mRNA is primarily expressed in epithelial cells (Epcam+ cells) at baseline (Figure 6A). Of note, although our IHC data in human lung showed no detectable ZIP8 staining on endothelial cells (CD31+), the sorted mouse lung endothelial cells expressed relatively high levels of *Zip8* mRNA, potentially because of contamination of the endothelial cell fraction with epithelial cells. We also found that sorted mouse alveolar macrophages (CD45+) express very low levels of *Slc39a8* mRNA (Figure 6A), in contrast to the splenic red pulp macrophages (Figure 2E).

As ZIP8 expression is very high in lung epithelial cells, we determined the directionality of iron transport by ZIP8 by treating ZIP8 KO and littermate controls with ^{58}Fe via RO injection into the bloodstream or OP aspiration into the airspace. After 4 hours, BAL fluid and lung tissue were harvested for ICP-MS analysis for ^{58}Fe. With RO ^{58}Fe, there was no difference in ^{58}Fe levels between ZIP8 KO mice and littermate controls in either BAL fluid or lung tissue. However, when ^{58}Fe was given OP, ZIP8 KO mice had more ^{58}Fe in the BAL fluid (fl/fl 54.97 ng vs KO 87.30 ng, $P = .097$) and less ^{58}Fe in the lung tissue (fl/fl 3160.13 ng vs KO 1823.77 ng, $P = .013$) compared with their controls (Figure 6B). These data indicate that ZIP8 functions to transport iron from the airspace into the lung. However, as we found no difference in steady-state lung iron levels between ZIP8 KO and littermate controls (Figure 6C), the import of iron from the air compartment likely does not play a large role in steady-state homeostasis. In addition, there was no difference in oxidative stress as measured by lung *Nqo1* mRNA and lung malondialdehyde (Figure 6D).

ZIP8 does not play a role in LPS-induced ALI

Because ZIP8 expression is induced by inflammation, we investigated whether ZIP8 plays a role in the response to inflammatory ALI. We treated 16-week-old ZIP8 KO mice and littermate controls with OP LPS 15 mg/kg or no treatment as previously described.[28] Based on our previous experience with this model, mice have particularly increased inflammatory parameters at day 3, so these mice were harvested after 3 days for BAL fluid and tissue analysis. LPS inflammation did induce ZIP8 expression in the lungs of wild-type mice (Figure 7A), but no difference was noted in lung nonheme iron levels between the ZIP8 KO mice and their controls (Figure 7B). Measurement of the ALI parameters of BAL protein and BAL/lung tissue MPO confirmed that LPS treatment resulted in significant lung injury, but ZIP8 deletion had no effect on the severity of ALI (Figure 7C-D). In addition, there was no change in

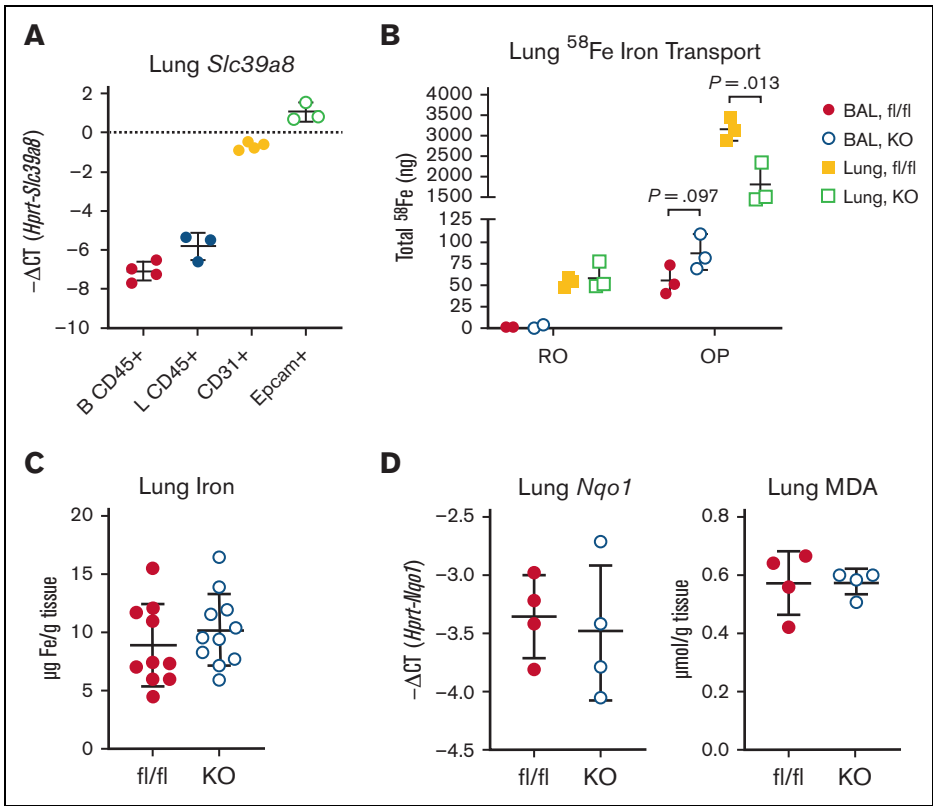

Figure 6. ZIP8 transports iron from the airspace into the lung. (A) *Slc39a8* mRNA levels of C57BL/6 mouse lung subpopulation cell types. B CD45+: BAL macrophages. L CD45+: lung macrophages. CD31+: endothelial cells. Epcam+: epithelial cells. n = 3 to 4 mice per group. (B) ZIP8 KO mice and littermate controls (fl/fl) were treated with 5 µg of $^{58}Fe^{2+}$ via RO injection or OP aspiration and harvested after 4 hours for ICP-MS analysis of ^{58}Fe levels. n = 3 mice per group. (C-D) 16-week-old ZIP8 KO and fl/fl mouse lung (C) nonheme iron levels and (D) *Nqo1* mRNA and MDA levels. n = 4 to 10 mice per group. (A-D) Graphs depict mean and SD; *P* values were determined by 2-tailed unpaired Student *t* test. MDA, malondialdehyde; SD, standard deviation.

oxidative stress as measured by mitochondrial SOD (Figure 7E). These data indicate that although lung ZIP8 is induced with inflammation, ZIP8 deletion does not modify the severity of LPS-induced ALI.

Loss of ZIP8 is protective against K. pneumoniae infection

Because ZIP8 is induced by inflammation, we hypothesized that ZIP8 may play a protective role in host defense by importing iron into the epithelium, thus lowering iron availability in the airspace. To test this, we administered OP 300 CFU of *K pneumoniae* in ZIP8 KO mice and controls, then analyzed the mice at 3 days after infection. Interestingly, ZIP8 KO mice experienced less weight loss than floxed littermate controls (fl/fl 15.53% vs KO 7.96%, $P = .0446$) and trended toward less bacterial burden in their lungs, livers, spleens, and blood as measured by CFUs (Figure 8A-B). There was no significant difference in lung injury as assessed by BAL protein and BAL protein and lung MPO levels (Figure 8C-D), and there was also no difference in oxidative stress, as measured by lung mitochondrial and cytosolic SOD (Figure 8E). Taken together, these data suggest that ZIP8 does not play a protective role in host defense and instead may worsen the outcomes of *K pneumoniae* infection through a yet unknown mechanism.

In summary, in our extensive characterization of global ZIP8 KO mice, we have shown that ZIP8 is highly expressed in the lung and can import iron into the epithelium from the air compartment. However, our data demonstrate that ZIP8 is not critical for lung iron homeostasis as evidenced by the analysis of baseline iron levels, although this interpretation is limited by the lack of cell-specific iron measurements in AT1 vs AT2 cells. ZIP8 also does not appear to play an important role in the inflammatory response to lung injury nor a protective host defense role against *K pneumoniae* lung infection. We have also demonstrated that ZIP8 is involved in splenic iron recycling; however, ZIP8 deletion alone is not sufficient to cause major hematological impairment at baseline or under stress conditions.

Discussion

In our examination of the role of ZIP8 in iron regulation, both systemically and in the lung, we generated many tools. As whole-body deletion of ZIP8 is embryonic lethal,[24,25] we generated an inducible ZIP8 KO mouse to allow for the study of the role of ZIP8 in an adult mouse model. In addition, we generated and validated a new anti-mouse ZIP8 antibody. This novel mouse model will potentially enable future studies of ZIP8 function in vivo.

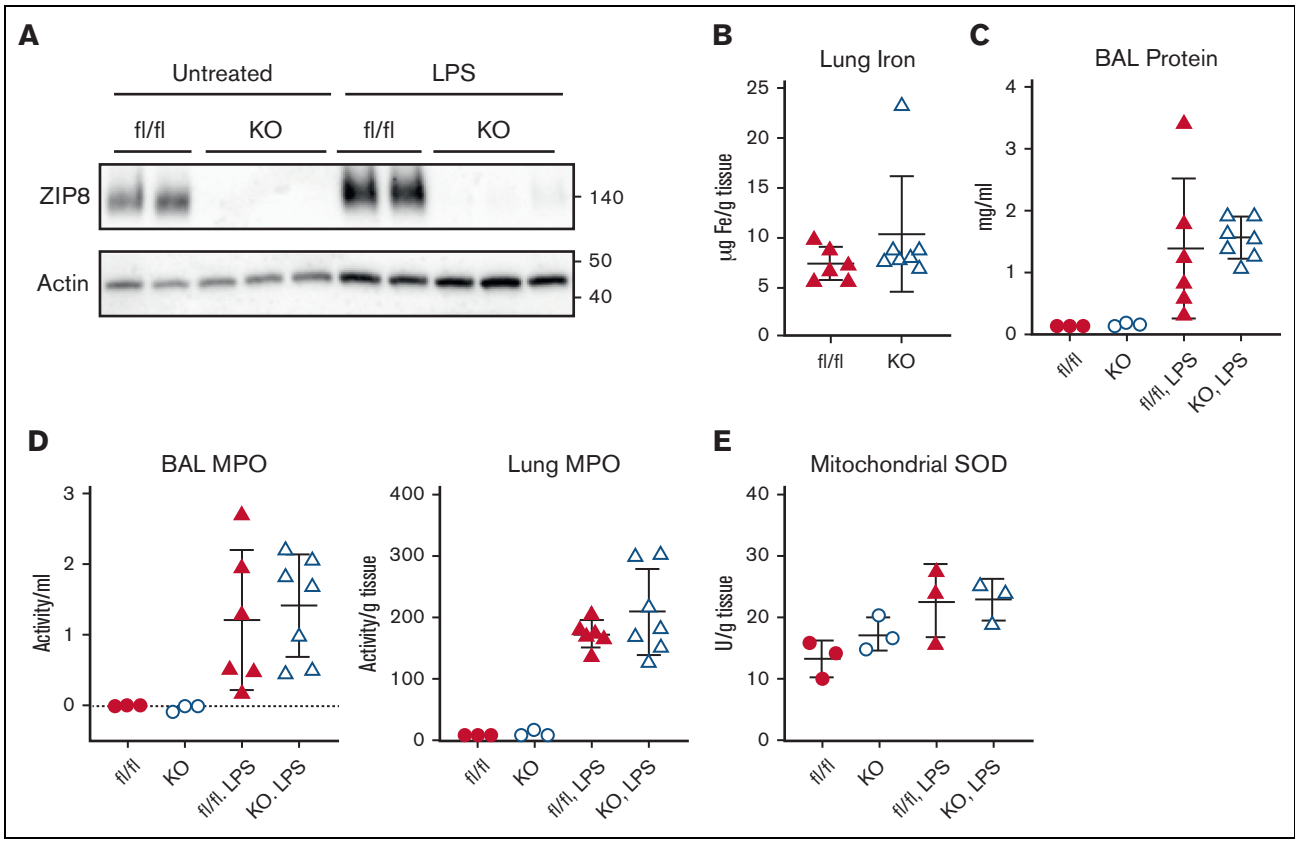

Figure 7. ZIP8 does not play a significant role in LPS-induced ALI. 16-week-old ZIP8 KO mice and littermate controls (fl/fl) were treated with 15 mg/kg LPS through OP aspiration to induce ALI and harvested after 3 days. A subset of mice in both groups were left untreated for comparison. n = 3 to 7 mice per group. (A) Representative western blot for ZIP8 in lung lysate. (B) Lung nonheme iron levels. (C) BAL protein levels. (D) BAL and lung tissue MPO activity. (E) Lung mitochondrial SOD. (B-E) Graphs depict mean and SD. SD, standard deviation.

Most of our findings regarding the role of ZIP8 in systemic iron regulation were replicated in 2 separate institutions with the same genetic mouse models, strengthening the validity of our findings. We did observe, however, some small differences between the 2 sets of mice. Increased splenic iron and decreased serum iron in ZIP8 KO mice at baseline were present in the findings of both labs. However lower baseline Hgb in ZIP8 KO mice compared with littermate controls was observed at UF but not at UCLA. Some changes in iron-handling proteins, such as ferroportin, TFR1, and ferritin, were also observed in 1 set of mice but not the other. A possible explanation could be the differences in vivarium environments, such as different diets or the use of metal cages, which could have altered iron bioavailability or the microbiome.

The increase in splenic iron in ZIP8 KO mice was primarily in the red pulp macrophages as determined by Perls' staining for iron, which suggests that ZIP8 is involved in iron recycling from RBCs. Erythrophagocytosis occurs when aged or damaged RBCs are hemolyzed and phagocytosed by red pulp macrophages in the spleen. The heme is released into the erythrophagosome and transported into the cytosol through HRG1.[29] HO-1 then breaks down heme and releases iron, which is then bound and stored in ferritin.[27] When the iron is needed, NCOA4 binds to and shuttles iron-laden ferritin to autophagosomes, which then fuse with lysosomes to break down ferritin and release the iron, which can then be exported from the cell through ferroportin.[30] We speculate that ZIP8 may be localized to an intracellular compartment and transport iron from within phagosomes (the erythrophagosome and/or autophagosome) to the cytosol, as indicated by the increase in iron in red pulp macrophages from ZIP8 KO mouse spleens. Despite this significant increase in splenic iron, however, we see minor or no effect on hematological parameters even after stressing the iron recycling system through hemolytic anemia or iron deficiency. In addition, we did not see any significant differences in splenic ferroportin, transferrin receptor, or ferritin levels under baseline conditions. This lack of effect of ZIP8 in iron recycling, despite the increased iron, may indicate redundancy with other intracellular transporters that could compensate for the loss of ZIP8. DMT1 is also expressed intracellularly, and natural resistance–associated macrophage protein 1, closely related to DMT1, is another intracellular iron transporter present in macrophages.[31,32] In addition, ZIP14, a metal transporter with a very similar structure to ZIP8, is also present in macrophages and is upregulated in activated macrophages.[14,33] It is possible that any of these could be upregulated and blunt the effects of ZIP8 deletion and iron sequestration on the body. The observation that splenic ZIP8 levels were markedly increased in response to hemolysis or iron dextran, both of which increase iron loading in red pulp macrophages,[34] suggests that splenic ZIP8 levels are regulated by iron. Furthermore, the increase in splenic ZIP8 levels was positively associated with

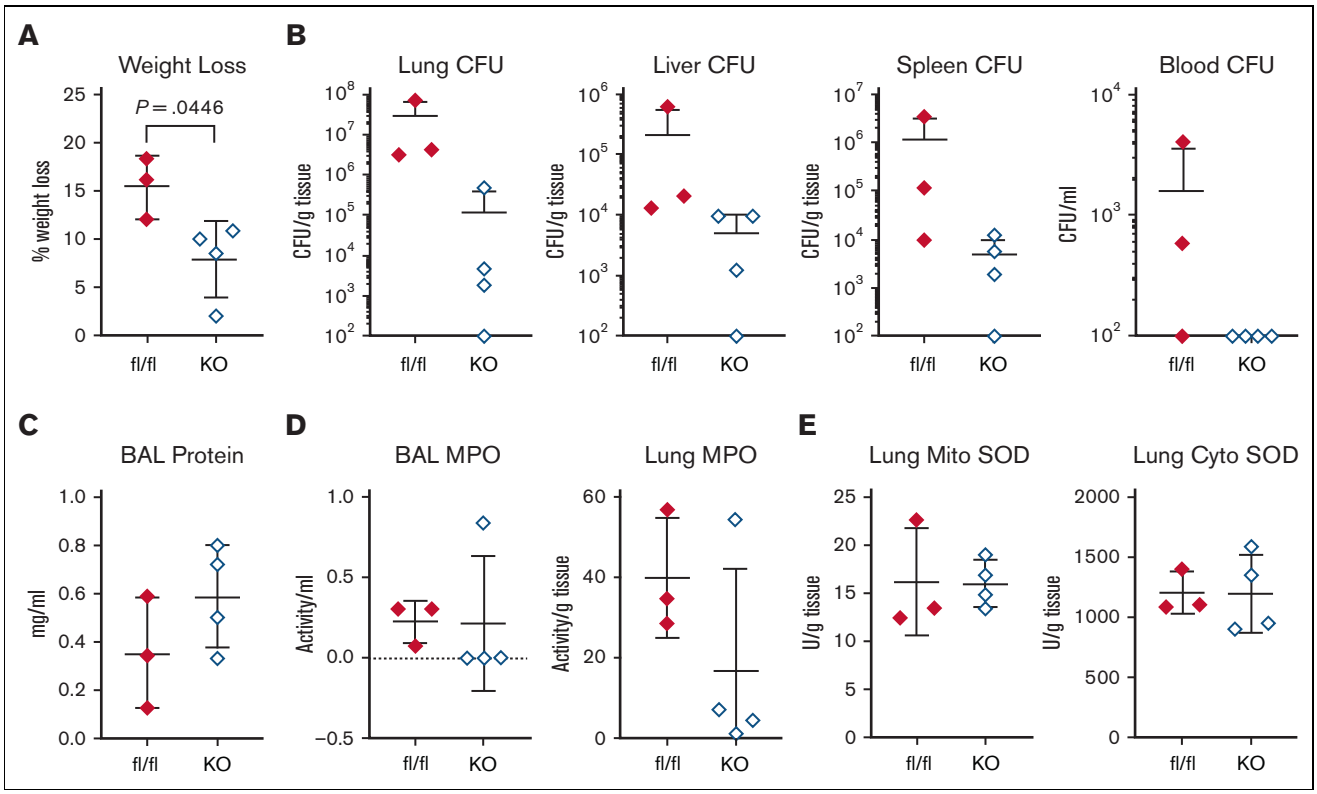

Figure 8. ZIP8 deletion is protective against *K pneumoniae* infection. ZIP8 KO mice and littermate controls (fl/fl) were infected with 1500 CFU of *K pneumoniae* via OP aspiration and weighed daily until harvest at 3 days. (A) Percent weight loss in ZIP8 KO and fl/fl mice. n = 3 to 4 mice per group. (B) CFU counts in lung, liver, spleen, and blood after infection. (C) BAL protein levels. (D) BAL and lung tissue MPO activity. (E) Lung mitochondrial and cytosolic SOD. Graphs depict mean and SD; *P* values were determined by 2-tailed unpaired Student *t* test. SD, standard deviation.

spleen iron content, suggesting a dose-response effect of iron loading on ZIP8 abundance, similar to what was found in cultured rat hepatoma cells.[15]

Regarding the role of ZIP8 in the lung, we have established that ZIP8 is expressed on the apical side of lung alveolar epithelial cells and confirmed that the direction of transport is from the airspace into the lung epithelium. Furthermore, we confirmed that ZIP8 expression is induced by LPS in mice and by IL-1a, IL-1b, and TNFα in A549 cells, a human lung epithelial cancer cell line. Though A549 cells are widely used to study alveolar epithelial cells,[35-37] a potential limitation of this study is the lack of confirmation using primary alveolar epithelial cells. Because inflammation-induced ZIP8 could sequester iron away from potential pathogens in the airspace, our initial hypothesis was that loss of ZIP8 would be detrimental during bacterial infections. However, loss of ZIP8 had no effect on response to ALI and we observed that loss of ZIP8 was actually beneficial in the case of *K pneumoniae* infection. This is in contrast to a recent publication by the Knoell group examining the role of ZIP8 in macrophages.[38] Their study demonstrated that loss of ZIP8, specifically in macrophages and dendritic cells, worsened pulmonary *Streptococcus pneumoniae* infection by hindering the immune response in a zinc-dependent manner through altered NF-κB signaling. One potential difference between our studies could simply be due to the differing pathogens used, as *K pneumoniae* is a gram-negative bacterium whereas *S pneumoniae* is gram-positive. Another difference could be the type of tissues where ZIP8 was deleted in the mouse models. Our mouse model was a whole-body postnatally-induced KO of ZIP8, which leads to loss of ZIP8 in the alveolar epithelium as well as macrophages and other cells. The mouse model used by the Knoell group specifically and constitutively knocks out ZIP8 in myeloid cells, which means that ZIP8 in the lung epithelium is still expressed. In addition, we found that ZIP8 is not expressed at baseline in alveolar macrophages, suggesting that the phenotype in the Knoell study may be related to the role of ZIP8 in monocyte-derived macrophages rather than specifically alveolar macrophages. Interestingly, a recent study by Liang et al[39] demonstrated the regulatory role of ZIP8 in the pathogenesis of idiopathic pulmonary fibrosis, indicating the potential importance of ZIP8 in other lung-specific pathologies. Altogether, our study indicates that ZIP8 does not appear to play a significant role in lung iron regulation nor a protective role in pulmonary host defense against *K pneumoniae* infection.

Although ZIP8 is highly expressed in the lung, our data on the lack of any major ZIP8 role in the lung are consistent with the reports of the human diseases where ZIP8 mutations are associated with nonpulmonary manifestations. In addition, although ZIP8 may not be critical for lung iron homeostasis or iron recycling, it may play a more important role in the transport of other divalent metals. ZIP8 has already been shown to be necessary for manganese uptake and recycling from the bile, and we have observed in our own mice that ZIP8 KO mice have significantly decreased manganese levels

(Lin et al[26], Figure 1). Furthermore, the human phenotype of ZIP8 loss has also been shown to be mostly related to manganese, as abnormal manganese homeostasis has been observed in human diseases such as schizophrenia, obesity, and Crohn's disease.[17-19] In addition, studies examining the role of ZIP8 in host defense characterized its effect as zinc-related and affecting the NF-κB pathway.[38,40,41]

Our study has shown that although ZIP8 may play a role in systemic iron recycling, as indicated by increased splenic iron in ZIP8 KO mice, it does not appear to have a significant role in pulmonary iron regulation or host defense. However, more remains to be learned about ZIP8 and iron regulation. One potential reason for the lack of significant iron-related differences in our ZIP8 KO mice is that ZIP8 may be most important during development, as complete loss of ZIP8 is embryonic lethal[24,25] and the placenta is the organ with the highest expression of ZIP8 after the lung.[15] As iron is critical for embryonic development,[42,43] ZIP8 may potentially play a greater role in iron regulation during development rather than in adulthood. Further studies are necessary to elucidate the role of ZIP8 during embryonic development.

Acknowledgments

The authors thank Borna Mehrad for generously providing formalin-fixed, deidentified normal human lung samples for this study. In addition, the authors thank the UC CEIN Inductively Coupled Plasma Mass Spectrometry Analysis Core and the UCLA Translational Pathology Core Laboratory for the services provided for this study.

The authors acknowledge financial support from the National Institutes of Health, National Heart, Lung, and Blood Institute R01 HL159507 (A.K.), and the National Institute of Diabetes and Digestive and Kidney Diseases R01 DK080706 (M.D.K.).

Authorship

Contribution: T.G., E.N., A.K., and M.D.K. conceived and designed the experiments; V.Z., S.J., A.K., Q.L., and M.D.K. performed experiments and prepared figures and the manuscript; and V.Z., T.G., E.N., A.K., Q.L., and M.D.K. analyzed the data and approved final version of the manuscript.

Conflict-of-interest disclosure: T.G. and E.N. are shareholders and scientific advisers of Intrinsic LifeSciences and Silarus Therapeutics, and consultants for Ionis Pharmaceuticals, Protagonist, Keryx Pharmaceuticals, La Jolla Pharma, Vifor, Akebia (T.G.), and Gilead (T.G.). M.D.K. has consulted for Pharmavite. A.K. has served on an advisory board for Pharmacosmos. The remaining authors declare no competing financial interests.

ORCID profiles: T.G., 0000-0002-2830-5469; E.N., 0000-0002-3477-2397; M.D.K., 0000-0001-9135-4696.

Correspondence: Airie Kim, David Geffen School of Medicine, 10833 LeConte Ave 43-229 CHS, Box 951690, Los Angeles, CA 90095; email: airiekim@mednet.ucla.edu.

References

1. Nemeth E, Ganz T. Hepcidin-Ferroportin Interaction Controls Systemic Iron Homeostasis. *Int J Mol Sci*. 2021;22(12):6493-6505.
2. Kosman DJ. A holistic view of mammalian (vertebrate) cellular iron uptake. *Metallomics*. 2020;12(9):1323-1334.
3. Vogt AS, Arsiwala T, Mohsen M, Vogel M, Manolova V, Bachmann MF. On Iron Metabolism and Its Regulation. *Int J Mol Sci*. 2021;22(9):4591-4607.
4. Delaby C, Rondeau C, Pouzet C, et al. Subcellular localization of iron and heme metabolism related proteins at early stages of erythrophagocytosis. *PLoS One*. 2012;7(7):e42199-e42211.
5. Ganz T. Iron and infection. *Int J Hematol*. 2018;107(1):7-15.
6. Stefanova D, Raychev A, Deville J, et al. Hepcidin Protects against Lethal Escherichia coli Sepsis in Mice Inoculated with Isolates from Septic Patients. *Infect Immun*. 2018;86(7):e00253-18-e00253-29.
7. Michels KR, Zhang Z, Bettina AM, et al. Hepcidin-mediated iron sequestration protects against bacterial dissemination during pneumonia. *JCI Insight*. 2017;2(6):e92002-e92014.
8. Stefanova D, Raychev A, Arezes J, et al. Endogenous hepcidin and its agonist mediate resistance to selected infections by clearing non-transferrin-bound iron. *Blood*. 2017;130(3):245-257.
9. Goetz DH, Holmes MA, Borregaard N, Bluhm ME, Raymond KN, Strong RK. The neutrophil lipocalin NGAL is a bacteriostatic agent that interferes with siderophore-mediated iron acquisition. *Mol Cell*. 2002;10(5):1033-1043.
10. Drago-Serrano ME, Campos-Rodriguez R, Carrero JC, de la Garza M. Lactoferrin: Balancing Ups and Downs of Inflammation Due to Microbial Infections. *Int J Mol Sci*. 2017;18(3).
11. Fritsche G, Nairz M, Libby SJ, Fang FC, Weiss G. Slc11a1 (Nramp1) impairs growth of Salmonella enterica serovar typhimurium in macrophages via stimulation of lipocalin-2 expression. *J Leukoc Biol*. 2012;92(2):353-359.
12. Zhang V, Nemeth E, Kim A. Iron in Lung Pathology. *Pharmaceuticals (Basel)*. 2019;12(1):30-40.
13. Ghio AJ, Soukup JM, Dailey LA, Madden MC. Air pollutants disrupt iron homeostasis to impact oxidant generation, biological effects, and tissue injury. *Free Radic Biol Med*. 2020;151:38-55.
14. Jenkitkasemwong S, Wang CY, Mackenzie B, Knutson MD. Physiologic implications of metal-ion transport by ZIP14 and ZIP8. *Biometals*. 2012;25(4):643-655.
15. Wang CY, Jenkitkasemwong S, Duarte S, et al. ZIP8 is an iron and zinc transporter whose cell-surface expression is up-regulated by cellular iron loading. *J Biol Chem*. 2012;287(41):34032-34043.

16. van Raaij SEG, Srai SKS, Swinkels DW, van Swelm RPL. Iron uptake by ZIP8 and ZIP14 in human proximal tubular epithelial cells. *Biometals*. 2019; 32(2):211-226.
17. Nebert DW, Liu Z. SLC39A8 gene encoding a metal ion transporter: discovery and bench to bedside. *Hum Genomics*. 2019;13(Suppl 1):51-71.
18. Sunuwar L, Frkatovic A, Sharapov S, et al. Pleiotropic ZIP8 A391T implicates abnormal manganese homeostasis in complex human disease. *JCI Insight*. 2020;5(20):e140978-e140990.
19. Costas J. The highly pleiotropic gene SLC39A8 as an opportunity to gain insight into the molecular pathogenesis of schizophrenia. *Am J Med Genet B Neuropsychiatr Genet*. 2018;177(2):274-283.
20. Galvez-Peralta M, Wang Z, Bao S, Knoell DL, Nebert DW. Tissue-Specific Induction of Mouse ZIP8 and ZIP14 Divalent Cation/Bicarbonate Symporters by, and Cytokine Response to, Inflammatory Signals. *Int J Toxicol*. 2014;33(3):246-258.
21. Pyle CJ, Akhter S, Bao S, Dodd CE, Schlesinger LS, Knoell DL. Zinc Modulates Endotoxin-Induced Human Macrophage Inflammation through ZIP8 Induction and C/EBPbeta Inhibition. *PLoS One*. 2017;12(1):e0169531-e0169549.
22. Knoell DL, Smith D, Bao S, et al. Imbalance in zinc homeostasis enhances lung Tissue Loss following cigarette smoke exposure. *J Trace Elem Med Biol*. 2020;60:126483-126492.
23. De Vooght V, Vanoirbeek JA, Haenen S, Verbeken E, Nemery B, Hoet PH. Oropharyngeal aspiration: an alternative route for challenging in a mouse model of chemical-induced asthma. *Toxicology*. 2009;259(1-2):84-89.
24. Wang B, He L, Dong H, Dalton TP, Nebert DW. Generation of a Slc39a8 hypomorph mouse: markedly decreased ZIP8 Zn(2)(+)/(HCO(3)(-))(2) transporter expression. *Biochem Biophys Res Commun*. 2011;410(2):289-294.
25. Chen J, Galvez-Peralta M, Zhang X, Deng J, Liu Z, Nebert DW. In utero gene expression in the Slc39a8(neo/neo) knockdown mouse. *Sci Rep*. 2018; 8(1):10703-10716.
26. Lin W, Vann DR, Doulias PT, et al. Hepatic metal ion transporter ZIP8 regulates manganese homeostasis and manganese-dependent enzyme activity. *J Clin Invest*. 2017;127(6):2407-2417.
27. Kovtunovych G, Eckhaus MA, Ghosh MC, Ollivierre-Wilson H, Rouault TA. Dysfunction of the heme recycling system in heme oxygenase 1-deficient mice: effects on macrophage viability and tissue iron distribution. *Blood*. 2010;116(26):6054-6062.
28. Zhang V, Ganz T, Nemeth E, Kim A. Iron overload causes a mild and transient increase in acute lung injury. *Physiol Rep*. 2020;8(12):e14470-e14479.
29. White C, Yuan X, Schmidt PJ, et al. HRG1 is essential for heme transport from the phagolysosome of macrophages during erythrophagocytosis. *Cell Metab*. 2013;17(2):261-270.
30. Bellelli R, Federico G, Matte A, et al. NCOA4 Deficiency Impairs Systemic Iron Homeostasis. *Cell Rep*. 2016;14(3):411-421.
31. Soe-Lin S, Apte SS, Andriopoulos B Jr, et al. Nramp1 promotes efficient macrophage recycling of iron following erythrophagocytosis in vivo. *Proc Natl Acad Sci U S A*. 2009;106(14):5960-5965.
32. Forbes JR, Gros P. Divalent-metal transport by NRAMP proteins at the interface of host-pathogen interactions. *Trends Microbiol*. 2001;9(8):397-403.
33. Giorgi G, D'Anna MC, Roque ME. Iron homeostasis and its disruption in mouse lung in iron deficiency and overload. *Exp Physiol*. 2015;100(10): 1199-1216.
34. Zhang Z, Zhang F, An P, et al. Ferroportin1 deficiency in mouse macrophages impairs iron homeostasis and inflammatory responses. *Blood*. 2011; 118(7):1912-1922.
35. Lieber M, Smith B, Szakal A, Nelson-Rees W, Todaro G. A continuous tumor-cell line from a human lung carcinoma with properties of type II alveolar epithelial cells. *Int J Cancer*. 1976;17(1):62-70.
36. Shapiro DL, Nardone LL, Rooney SA, Motoyama EK, Munoz JL. Phospholipid biosynthesis and secretion by a cell line (A549) which resembles type II aleveolar epithelial cells. *Biochim Biophys Acta*. 1978;530(2):197-207.
37. Wu J, Wang Y, Liu G, et al. Characterization of air-liquid interface culture of A549 alveolar epithelial cells. *Braz J Med Biol Res*. 2017;51(2):e6950-e6958.
38. Hall SC, Smith DR, Dyavar SR, et al. Critical Role of Zinc Transporter (ZIP8) in Myeloid Innate Immune Cell Function and the Host Response against Bacterial Pneumonia. *J Immunol*. 2021;207(5):1357-1370.
39. Liang J, Huang G, Liu X, et al. The ZIP8/SIRT1 axis regulates alveolar progenitor cell renewal in aging and idiopathic pulmonary fibrosis. *J Clin Invest*. 2022;132(11):e157338-e157353.
40. Liu MJ, Bao S, Galvez-Peralta M, et al. ZIP8 regulates host defense through zinc-mediated inhibition of NF-kappaB. *Cell Rep*. 2013;3(2):386-400.
41. Pyle CJ, Azad AK, Papp AC, Sadee W, Knoell DL, Schlesinger LS. Elemental Ingredients in the Macrophage Cocktail: Role of ZIP8 in Host Response to Mycobacterium tuberculosis. *Int J Mol Sci*. 2017;18(11):2375-2390.
42. Sangkhae V, Fisher AL, Wong S, et al. Effects of maternal iron status on placental and fetal iron homeostasis. *J Clin Invest*. 2020;130(2):625-640.
43. Fisher AL, Sangkhae V, Presicce P, et al. Fetal and amniotic fluid iron homeostasis in healthy and complicated murine, macaque, and human pregnancy. *JCI Insight*. 2020;5(4):e135321-e135334.